Arabian Journal of Chemical and Environmental Research

Vol. 07 Issue 1 (2020) 12–28

Kinetics and thermodynamic modelling of natural and synthetic goethite for dyes scavenging from aqueous systems

F.A. Ugbe[1*] and N. Abdus-Salam[2]

[1]*Department of Chemistry, Faculty of Physical Sciences, Ahmadu Bello University, P.M.B. 1044, Zaria, Nigeria.*

e-mail: ugbefabianaudu@gmail.com

[2]*Department of Chemistry, Faculty of Physical Sciences, University of Ilorin, P.M.B. 1515, Ilorin, Nigeria.*

e-mail: nasalami2002@yahoo.co.uk

Received 12 July 2020, Revised 30 July 2020, Accepted 31 July 2020

Abstract

In order to significantly understand the mechanism of fixation of dyes onto goethite surfaces, the kinetics and thermodynamic properties of natural goethite (NGT) and synthetic goethite (SGT) for methylene blue (MB) and eosin yellow (EY) adsorption was investigated. Batch equilibrium assay was used to study the influence of agitation time and temperature on the adsorption efficiency, results of which showed that the adsorption processes were dependent on both equilibrium parameters, with SGT exhibiting relatively higher adsorption capacity. The experimental data were fitted into some kinetics models (pseudo-first order, pseudo-second order, second order, Elovich, intra-particle diffusion (Weber-Morris), and film diffusion) while some thermodynamic parameters such as ΔG, ΔH, ΔS and isosteric heat of adsorption (ΔHr) were evaluated. The orders of fittings are pseudo-second order (R^2 = 1) > Elovich (0.9717) > second order (0.9579) > pseudo-first order (0.8737), and Weber-Morris (0.9117) > film diffusion (0.8737). Thermodynamics study showed that the adsorption was feasible, spontaneous (all ΔG values are negative) and exothermic (except MB-NGT with ΔH = +0.538kJ/mol) in nature. Combined results of kinetics and thermodynamics studies suggested a combined chemisorptions and physisorptions processes as revealed by best fitting model (pseudo-second order) and magnitudes of ΔH (range of 20.9 – 80kJ/mol for EY and < 20.9kJ/mol for MB adsorption) and ΔHr (> 40kJ/mol for EY and < 40kJ/mol for MB removal). Furthermore, the diffusion models suggested that intra-particle and film diffusion occurred simultaneously or in combination with other processes in the mechanism of adsorption.

Keywords: Adsorption, natural goethite, synthetic goethite, eosin yellow, methylene blue.

*Corresponding author. *E-mail address:* ugbefabianaudu@gmail.com

1. Introduction

Water pollution has become increasingly worrisome since water constitutes a basic necessity of life and thus, key to survival of all living organisms on the planet earth [1]. This problem is increasing with developing technology; dye pollution is one of the main problems [2]. In developing countries such as Nigeria, notable industries responsible for the release of large volume of dye effluents into water system include amongst others textiles, food, polymers, and cosmetic industries [3]. Dyes present in effluents are non-biodegradable and carcinogenic in nature [4]. High concentration of dyes in water bodies significantly reduce the oxygenation capacity of receiving water and prevent it from accessing sunlight thus making it difficult for survival in the aquatic environment [5]. Dyes may accumulate in human body once they get into the human food chain and have the potentials of causing severe health problems if they exceed their permissible limits [2]. Some health complications associated with ingestion of water containing dyes include shock, diarrhoea, jaundice, allergies, skin irritation, or different tissue changes etc [5-6].

It is therefore essential that the water reserves be treated carefully and wastewater treatment carried out effectively [7]. Researchers have used many techniques for treatment of dye wastewater, such as advance oxidation, flocculation, biodegradation, photo-degradation, electrodialysis, and membrane filtration [4], [8-9]. These techniques have one form of limitation or the other including cost ineffectiveness, non-availability, and low efficiency [3], which are not associated with adsorption technique [10-11]. Thus, different adsorbents have been developed and used for the removal of dyes and other organics in wastewater such as fir bark [6], pineapple peels [7], *Ocimum gratissimum* [3], tea waste [12], *Metroxylon spp*. waste [13], termite mound [14], bentonite [15], coconut husks [16] etc. In the continuous search for novel adsorbents suitable for effective scavenging of non-biodegradable pollutants from waste water, the properties of natural goethite (NGT) and synthetic goethite (SGT) for adsorption of eosin yellow (EY) and methylene blue (MB) dyes from aqueous system was investigated. Figure 1(a-b) shows the chemical structures of both dyes.

Iron ore deposits have been found in various locations in Nigeria, but mainly in the north-central, north-east, and south-east regions, majorly in the form of goethite, hematite, magnetite, limonite, maghemite, and siderite [17]. Goethite (FeO(OH)), is an iron mineral containing the hydroxy group which makes it easier to bind strongly to both organic and inorganic ligands [18]. It equally shows high specific surface areas and strong affinities for surface binding [19], thereby making it a choice of adsorbent in this study. Synthesized goethite when compared with their naturally occurring counterparts has an improved purity and tailored composition with desired surface properties and particle size [20].

Therefore, the kinetics and thermodynamic properties of goethite for sorption of MB and EY was investigated to provide insights into the feasibility and mechanisms of fixation of these dyes onto

goethite surfaces, while also taking note of the adsorption efficiencies of both adsorbents for the dyes uptake.

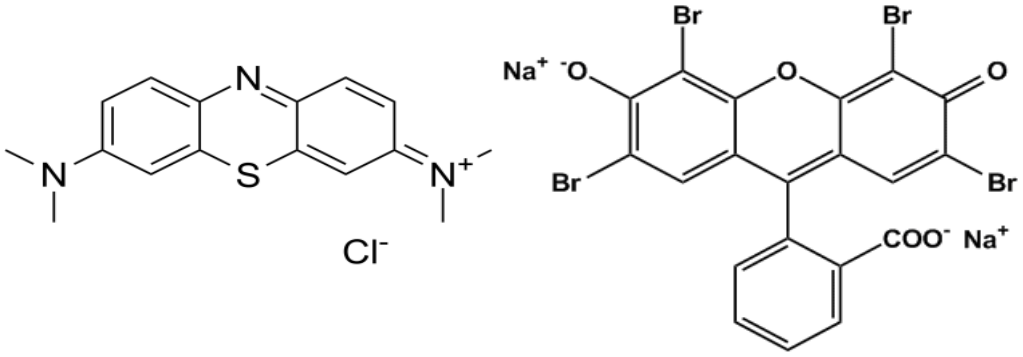

(a) **(b)**

Fig 1. Chemical structure of (a) MB and (b) EY

2. Materials and Methods

2.1. Preparation and characterization of adsorbents

Sample of NGT used in this study was obtained from the National Iron Ore Mining Company (NIOMCO), Itakpe, Kogi State, Nigeria, while SGT (α-FeOOH) was synthesized in the laboratory according to the method reported by Lee *et al*. [21]. Both Samples were then prepared and characterized using the following instrumental methods: X-ray fluorescence (XRF) for elemental compositions of the adsorbents, Fourier Transform Infrared Spectrometry (FTIR) for surface functional groups, Scanning Electron Microscopy (SEM) for grain size and morphological properties, Brauner-Emmet-Teller Isotherm (BET) for surface area determination (for SGT only), and nano-sizing for nano-size determination (for SGT only). An experiment to determine the point of zero charge (pHpzc) was also conducted on both adsorbents. The results of the various investigations were however published separately by Abdus-Salam *et al* [22].

2.2. Adsorption experiment

Batch mode adsorption study was carried out to investigate the effect of time and temperature on the sorption of MB and EY onto NGT and SGT. 15 ml solution each of MB and EY at constant optimum concentration (200ppm MB-NGT, 250ppm MB-SGT, 150ppm EY-NGT, and 200ppm EY-SGT) and pH (10 for MB and 2 for EY) earlier obtained from optimization experiment, were contacted with both adsorbents (0.5 g NGT of particle size 0.112 mm and 0.1g SGT of size 172.5nm) in separate 100 ml capacity conical flask prepared for the various unique systems. The various flasks and its content were

agitated on an orbital mechanical shaker at varying times (5, 10, 20, 30, 45, 60, 90 and 120) minutes for effect of time and at varying temperatures (303, 308, 313, 318 and 323) K for 2hrs for thermodynamic study. Each solution was then filtered and the filtrates analyzed for dye using UV-Visible spectrophotometer at a predetermined wavelength of maximum absorption (λ_{max}) of 668nm for MB and 517nm for EY [23-24]. Note that the different masses of both adsorbents used was that which enabled their easy handling and more so that the quantity adsorbed is always normalized by the mass of the adsorbent to allow comparison between two or more adsorbent materials.

The dye quantities adsorbed by the adsorbents at equilibrium were determined using the mass balance equation (eqn 1) [25].

$$q_e = \frac{V(C_i - C_e)}{m} \qquad \text{equation 1}$$

Where q_e is the dye concentration adsorbed on the adsorbent at equilibrium (mg/g), v is the initial volume of dye in solution (L), C_i and C_e is the initial concentration and equilibrium concentration of dye in the solution (mg/L) respectively, and m is the mass of the adsorbent used (g).

The experimental results were fitted into six kinetics models; pseudo-first order, pseudo-second order, second order, Elovich, intra-particle diffusion (Weber-Morris) and film diffusion, while some basic thermodynamic parameters such as Gibb's free energy change (ΔG), enthalpy change (ΔH), entropy change (ΔS) and isosteric heat of adsorption (ΔHr) were evaluated. The various equations and parameters are presented in Table 1.

3. Results and discussion

3.1. Characterization

The result of characterization of the adsorbents was reported elsewhere [22]. From the results, the pH_{pzc} was found to be 7.0 and 8.0 for NGT and SGT respectively. FTIR analysis revealed OH as the major functional group on both adsorbents. SGT exhibited a high porosity and more regular shapes of particles than NGT as revealed by SEM analysis. The main elemental composition of both goethite forms was iron with percentage composition by mass of 66.1930% and 66.4009% for NGT and SGT respectively as obtained from XRF analysis. Furthermore, the BET analysis showed SGT surface area of 797.662 m^2/g, whilst the size of SGT particles predominantly fall within 172 – 173 nm which are near nano-scale [22].

3.2. Effect of time

The effect of time on the adsorption of MB and EY was studied between 5 and 120 minutes at constant optimum concentration and pH. Table 2 illustrate adsorption of the dyes at different time duration.

Table 1. Some adsorption kinetics and thermodynamics equations with their parameters

Model	Equation	Linear plot	Eqn.	Author(s)
Pseudo first order	$\ln(q_e - q_t) = \ln q_e - k_1 t$	$\ln(q_e - q_t)$ vs t Slope: $-k_1$ Intercept: $\ln q_e$	2	[26]
Pseudo second order	$\frac{t}{q_t} = \frac{1}{k_2 q_e^2} + \left(\frac{1}{q_e}\right) t$	t/q_t vs t Slope: $1/q_e$ Intercept: $1/k_2 q_e^2$	3	[27]
Second order	$\frac{1}{C_t} = k_2 t + \frac{1}{C_e}$	$1/C_t$ vs t Slope: k_2 Intercept: $1/C_e$	4	[28]
Elovich	$q_t = \propto \ln(a \propto) + \propto lnt$	q_t vs lnt Slope: α Intercept: $\alpha ln(a\alpha)$	5	[29]
Intra-particle diffusion	$q_t = k_{id} t^{\frac{1}{2}} + C$	q_t vs $t^{1/2}$ Slope: k_{id} Intercept: C	6	[30]
Film diffusion	$\ln\left[1 - \frac{q_t}{q_e}\right] = -R^1 t + C$ $R^1 = \frac{3D_e^1}{r_0 \Delta r_0 K'}$	$\ln\left[1 - \frac{q_t}{q_e}\right]$ vs t Slope: $-R^l$ Intercept: C	7	[31]
Van't Hoff	$lnK_C = \frac{\Delta S}{R} - \frac{\Delta H}{RT}$ $K_C = \frac{C_S}{C_e}$ $\Delta G = \Delta H - T\Delta S$	$ln\ K_c$ vs 1/T Slope: $-\Delta H/R$ Intercept: $\Delta S/R$	8	[32-33]
Clausius-Clapeyron	$lnC_e = -\left(\frac{\Delta H_r}{R}\right)\frac{1}{T} + K$	lnC_e vs 1/T	9	[34]

Kinetics

q_e = ads capacity ($mg.g^{-1}$) at equil
k_1 = pseudo 1st order rate constant (min^{-1})
k_2 = pseudo 2nd order rate constant (g/ mg/min)
q_t = ads capacity at time, t ($mg.g^{-1}$)
t = time (min)
k_2 = second-order rate constant (L/(mg·min))
a = desorption constant
α = initial ads rate
C_e = conc of solute at equil (mg/L)
C_t = conc of solute at time, t (mg/L)
C = describes the boundary layer thickness
k_{id} = intra-particle diffusion rate constant ($mg/g/min^{1/2}$)
R^l = Liquid film diffusion constant (min^{-1})
D_e^l = effective liquid film diffusion coefficient (cm^2/min)
r^0 = radius of adsorbent beads (cm)
Δr^0 = thickness of liquid film (cm)
K′ = ads equil constant

Thermodynamics

ΔH = enthalpy change ($Jmol^{-1}$)
ΔS = entropy change ($Jmol^{-1}K^{-1}$)
ΔG = Gibb's free energy change ($Jmol^{-1}$)
R = Molar gas constant (8.314 $Jmol^{-1}K^{-1}$)
T = temperature (K)
K_c = conc equil constant
C_s = conc of analyte on the adsorbent at equil (mgL^{-1})
C_e = conc of analyte in bulk solution at equil (mgL^{-1})

ads = adsorption, equil = equilibrium, conc = concentration

Table 2 revealed there was fast uptake of these dyes as agitation time was increased from 5 minutes and reached equilibrium at 60 minutes for MB-NGT (0.051 mg/g, 98.35%), EY-NGT (4.496 mg/g, 99.90%) and 90 minutes for MB-SGT (33.20 mg/g, 88.51%), and EY-SGT (39.92 mg/g, 99.80%). The adsorption

of both dyes on the adsorbents was generally characterized by a rapid adsorption within the first 5 min of contact. i.e. 84.48% MB and 99.30% EY were adsorbed by SGT while NGT adsorbed 97.89% MB and 99.51% EY within the same time. Further increment in the time of contact resulted to only a slight increase in uptake until equilibrium was attained, after which the adsorption was then later slowed down with minimal incremental adsorption for both dyes on NGT. This is the general characteristic of adsorption of various adsorbates on iron oxides [23], [35].

Table 2. Data for quantity adsorbed as function of +time for sorption of MB and EYonto NGT and SGT

t (min)	$q_{e,exp}$ (mg/g)			
	MB		EY	
	NGT	SGT	NGT	SGT
5	0.024	31.68	4.478	39.72
10	0.047	31.98	4.482	39.75
20	0.025	32.29	4.487	39.79
30	0.041	32.74	4.485	39.86
45	0.050	32.93	4.484	39.87
60	0.051	33.15	4.496	39.89
90	0.049	33.20	4.487	39.92
120	0.047	33.20	4.487	39.92

Generally, the adsorbate adsorption takes place at the more reactive surface sites. As these sites are progressively filled the more difficult the sorption becomes, as the sorption experiment tends to be more unfavourable. This is as a result of saturation of adsorption sites of goethite at higher contact time [36]. Also the quantities of all adsorbates taken by SGT were relatively higher. This may be due to the fact that SGT, an iron compound contains relatively higher proportion of pure goethite particles per unit mass of sample used, rather than greater chemical reactivity of the synthetic goethite. Similar observation was been reported elsewhere [23].

3.3 Adsorption kinetics and mechanism analysis

The knowledge of the kinetics of adsorption processes helps to determine the rate at which solute molecules from the bulk solution are taken up onto the surface of the adsorbents, the rate determining steps, as well as the mechanism of the adsorption [37-38]. Consequently, the kinetics of the adsorption of MB and EY onto both goethite forms was studied from the variation of agitation time experiment using Pseudo-first order, pseudo-second order, second order, Elovich, Weber-Morris and film diffusion models, and the results were presented in Table 3 and Figures 2-4.

Table 3. The adsorption kinetics parameters for MB and EY onto NGT and SGT

Adsorption Kinetics	$q_{e,exp}$ (mg/g)	Pseudo-first order			Pseudo-second order		
		K_1 (min^{-1})	$q_{e,cal}$ (mg/g)	R^2	k_2 (g/mg/min)	$q_{e,cal}$ (mg/g)	R^2
MB - NGT	0.051	0.0286	0.00409	0.0767	3.892	0.0507	0.9848
MB - SGT	33.20	0.101	7.797	0.8737	0.066	33.33	1
EY - NGT	4.496	0.0073	0.014	0.192	709.14	4.488	1
EY - SGT	39.92	0.0821	0.92	0.8507	0.446	40	1

-	Second order			Elovich		
	k_2	C_e (mg/L)	R^2	a	α	R^2
MB - NGT	4.00E-04	3.817	0.3546	1514.08	0.0072	0.5388
MB - SGT	8.00E-05	36.232	0.7679	2.70E+25	0.5321	0.9627
EY - NGT	0.01	0.469	0.0522	-	0.0028	0.3996
EY - SGT	1.80E-02	1.417	0.9579	-	0.0702	0.9717

-	Weber-Morris			Film diffusion	
	k_{id}	C	R^2	R^1	R^2
MB - NGT	0.0024	0.0271	0.4531	0.0286	0.0769
MB - SGT	0.1823	31.501	0.8728	0.101	0.8737
EY - NGT	0.0009	4.4805	0.2866	0.0073	0.1920
EY - SGT	0.0245	39.688	0.9117	0.0821	0.8507

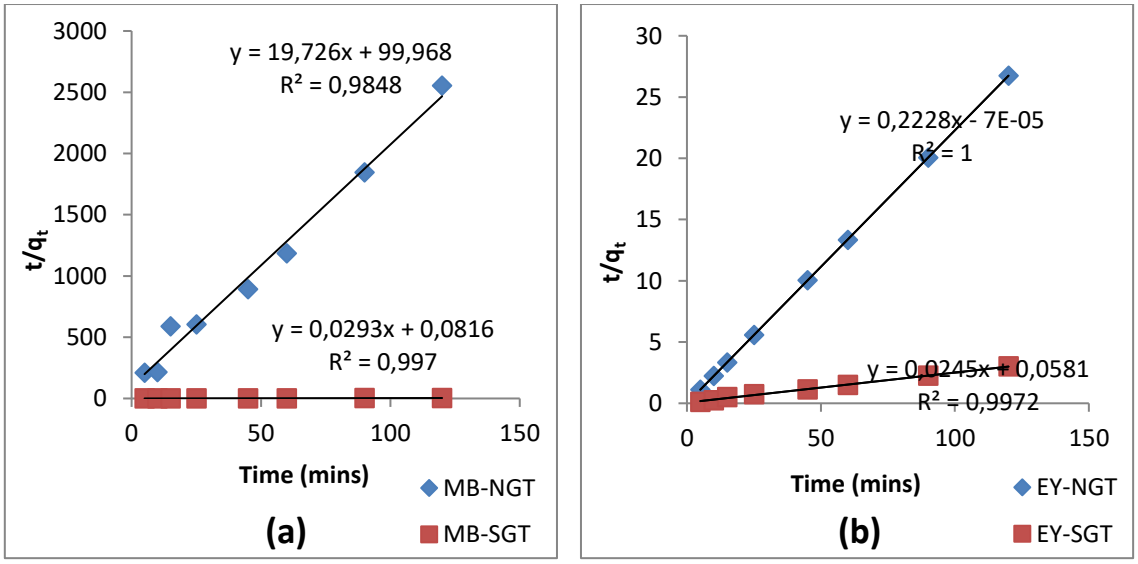

Fig 2. Pseudo second order plot for sorption of (a) MB and (b) EY, onto NGT and SGT.

The results of kinetics study shown in Tables 3 revealed the order of fittings; pseudo-second order > Elovich > second order > pseudo-first order for all dye-adsorbent systems studied. The pseudo-first order model was only fairly obeyed in MB-SGT (R^2 = 0.8737) and EY-SGT (0.8507). This model showed poor fittings to sorption of these dyes onto NGT, having R^2 values far less than one (0.0767 for MB and 0.192 for EY).

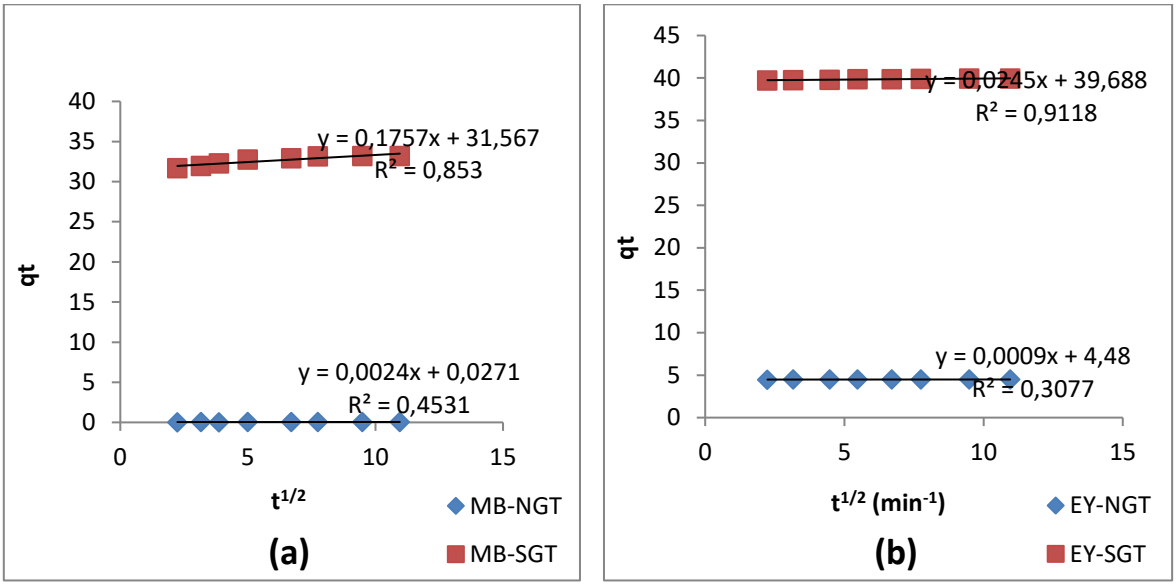

Fig 3. Weber-Morris plot for sorption of (a) MB and (b) EY, onto NGT and SGT.

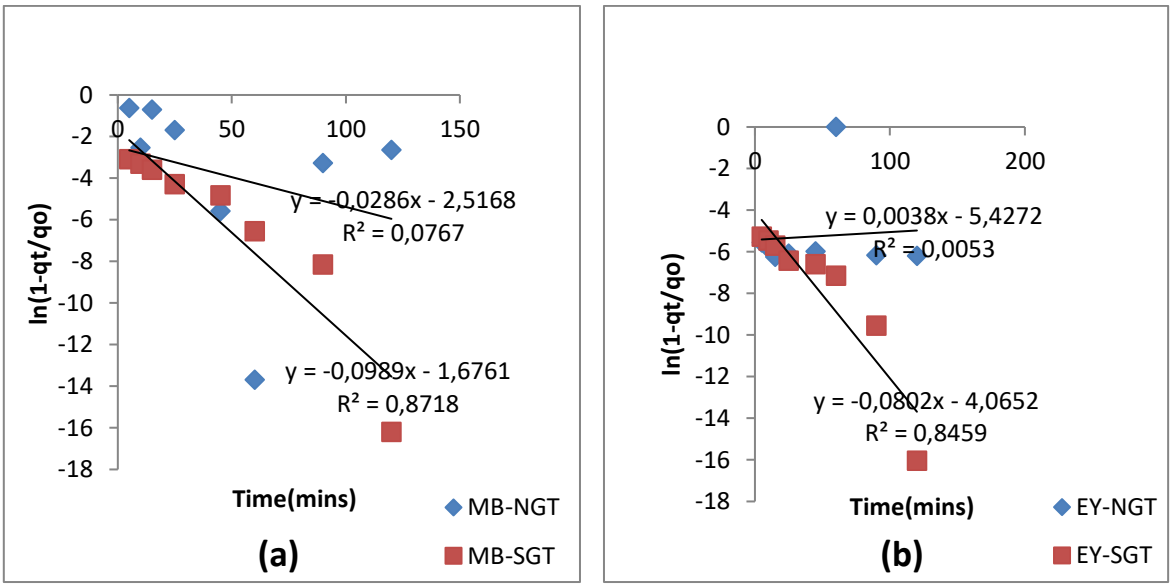

Fig 4. Film diffusion plot for sorption of (a) MB and (b) EY, onto NGT and SGT.

More so, there exist great discrepancy between the experimentally obtained q_e ($q_{e,exp}$) and that obtained from the kinetics equation ($q_{e,cal}$), which revealed that pseudo-first order model could not describe the kinetic data for adsorption of the dyes onto both goethite adsorbents. Similar observation was earlier reported by Dada *et al.* [3], Edet and Ifelebuegu [39], and Borah *et al.* [12], which are in agreement with the fact that most liquid phase adsorption processes do not fit into pseudo-first order model. Pseudo-second order model on the other hand shows the significance of the type of bonding that coexists between adsorbents and adsorbates during adsorption, it assumes chemisorptions (covalent or ionic bonds) as the rate controlling step through the sharing of the valence electrons [40]. The adsorption processes fitted perfectly into the pseudo-second order model with most of the R^2 values been one (the least is 0.9848).

The closeness of the experimentally obtained q_e ($q_{e,exp}$) and that obtained from the kinetics equation ($q_{e,cal}$) for all dye-adsorbent systems further supported the finding that the processes were adequately described by pseudo-second order model, indicating that the adsorption processes proceeded by chemisorption mechanism. Similar result was earlier reported by Adegoke *et al*. [41] and Eman *et al*. [42]. Comparison of equilibrium adsorption capacities ($q_{e,cal}$) obtained from pseudo-second order equation with those of other adsorbent materials is shown at Table 4.

Second order and Elovich like the pseudo-second order model corroborates the chemisorption process of adsorption [43]. Elovich model describes uniquely the heterogeneity of the adsorbent surface and posits that the rate of adsorption decreases exponentially with time due to increase coverage on the surface of the adsorbents [29], [44-45]. It was observed from Table 3 that the second order and Elovich models fitted well the adsorption of these dyes onto SGT than NGT, with the R^2 values obtained for Elovich being relatively higher. This further supports the fact that the adsorption processes onto SGT is chemisorption in nature.

Table 4. Comparison of equilibrium adsorption capacities for different adsorbent materials

Adsorbent	q_e (mg/g)		Author (s)
	MB	EY	
Biochar	42.92	-	[48]
Biochar/Fe_xO_y	86.29	-	[48]
Raw date seed	2.187	-	[49]
Roasted date seed	4.48	-	[49]
Carbon from tea waste	400	384.54	[12]
Termite mound	11.86	-	[14]
Pineapple peels	-	21.73	[7]
NGT	0.051	4.482	This study
SGT	33.33	40	This study

The mechanism of any adsorption process may proceed either by adsorption onto the external surface of the adsorbent (film diffusion) and/or adsorption into the internal pores of the adsorbent (intra-particle diffusion) [46]. The linearity of these models to any given experimental data shows the good applicability and the determination of the rate controlling step(s) in the adsorption process [47]. As shown in Table 3, it was observed that the intra-particle diffusion model fitted the sorption data better than film diffusion model. Both models fitted well the adsorption process of the dyes onto SGT than NGT with the highest R^2 value observed for EY-SGT (0.9117) and the lowest with MB-NGT (0.0769). Also, the plots of both models failed to pass through the origin (Figures 3-4). This signifies that none of

the models is the sole rate limiting step in the adsorption processes or that other processes occurred simultaneously with these two processes in the mechanism of the adsorption [38].

In conclusion to the kinetic studies of the adsorption of MB and EY onto NGT and SGT; the fittings are in the order: pseudo-second order > Elovich > second order > pseudo-first order. The adsorption proceeded by a chemisorption process as suggested by the Pseudo-second order, Elovich and second order models, and that the mechanism of the adsorption occurred by the two processes (intra-particle and film diffusion) simultaneously as the rate controlling steps or that other processes occurred simultaneously with these two processes in the mechanism of the adsorption.

3.4. Thermodynamic study

In order to fully understand the nature of the adsorption, some thermodynamic parameters such as Gibb's free energy change (ΔG), enthalpy change (ΔH), entropy change (ΔS), and isosteric heat of adsorption (ΔH_r) were calculated from the data generated from the variation of temperature experiment. The results of thermodynamics parameters and plots for the adsorption of MB and EY onto NGT and SGT were presented in Table 5 and Figures 5-6 respectively.

Table 5. Thermodynamics parameters for the sorption of MB and EY onto NGT and SGT

Adsorption Thermodynamics	Parameters					
	T (K)	q_e (mg/g)	ΔG (kJ/mol)	ΔS (J/mol.K)	ΔH (kJ/mol)	ΔHr (kJ/mol)
MB - NGT	303	5.027	-4.14	15.42	0.538	-0.451
	308	5.029	-4.21			
	313	5.030	-4.28			
	318	5.034	-4.36			
	323	5.038	-4.44			
MB - SGT	303	32.79	-4.89	-0.835	-5.146	4.46
	308	32.67	-4.89			
	313	32.52	-4.88			
	318	32.41	-4.89			
	323	32.24	-4.87			
EY - NGT	303	4.495	-16.96	-197.66	-76.39	76.11
	308	4.488	-15.12			
	313	4.481	-14.18			
	318	4.472	-13.43			
	323	4.464	-12.91			
EY - SGT	303	29.92	-15.05	-90.45	-42.42	42.23
	308	29.9	-14.5			
	313	29.87	-14.18			
	318	29.83	-13.61			
	323	29.78	-13.24			

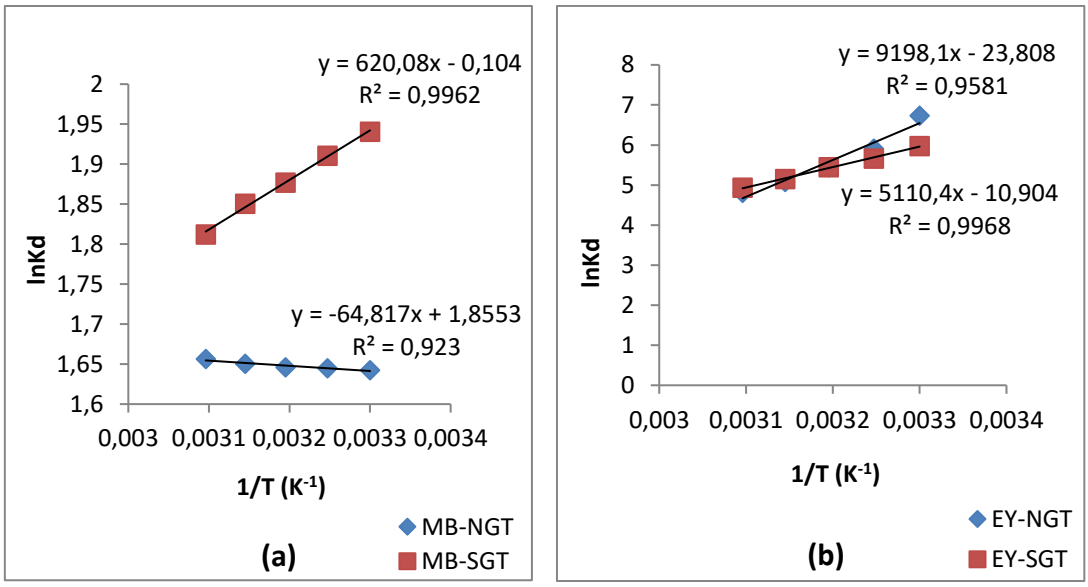

Fig 5. Thermodynamic plot (Van't Hoff) for the sorption of (a) MB and (b) EY, onto NGT and SGT.

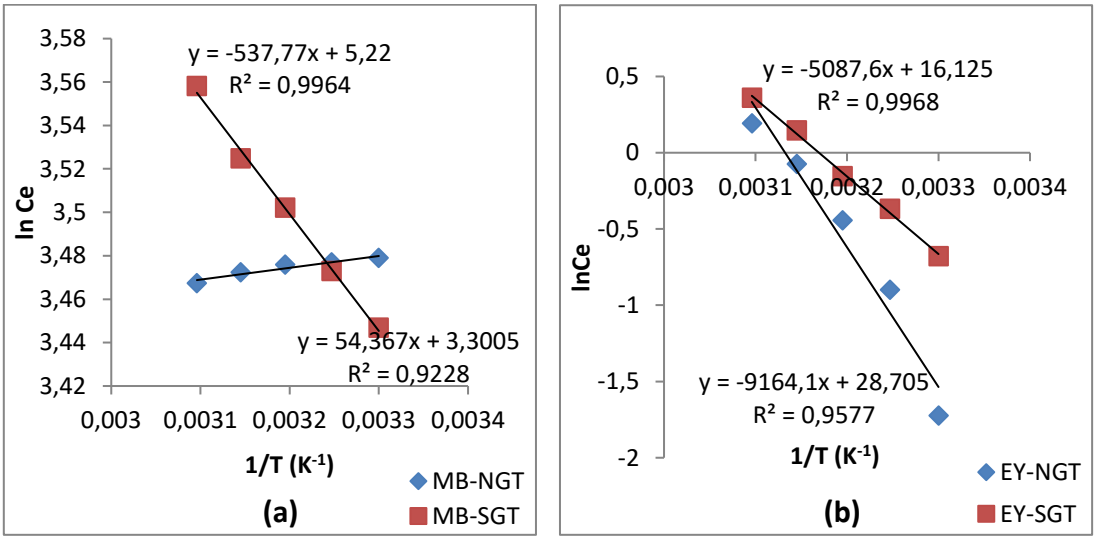

Fig 6. Thermodynamic plot (Clausius Clapeyron) for the sorption of (a) MB and (b) EY, onto NGT and SGT.

As seen from Tables 5, the values of the ΔG are all negative. This indicates the feasibility and spontaneity of the adsorption process for the range of temperature tested. Similar result was reported by Ugbe *et al*. [32], Muhammad *et al*. [1], Ladan *et al*. [24] and Boparai *et al*. [50]. Also, ΔG became decreasingly negative with tempertaure for the sorption of EY onto the adsorbents; an indication that adsorption is more favourable as solution temperature is lowered (exothermic process). This is attributed to the fact that at higher temperature, the physical interaction between the adsorbates and the adsorbent became

weaker. Similar results have been reported by Prabakaran and Arivoli [51], Rattanaphani *et al*. [52] and Chartterjee *et al*. [53].

The positive values of enthalpy change (ΔH) (Table 5) for MB-NGT confirmed that the process is endothermic; as evident in the slightly enhanced removal at increased temperature. Opposite trend was observed for MB-SGT, EY-NGT and EY-SGT as values of enthalpy change are negative; an indicative of exothermic process [34]. The magnitude of ΔH values for the sorption of EY onto both adsorbents fall into the range of 20.9–80 kJ/mol, an indicative of combined physisorption and chemisorptions mechanism at work. Adsorption of MB onto the adsorbents has enthalpy changes below 20.9 kJ/mol, indicating physical adsorption [1], [32], [34].

Positive value of entropy change (ΔS) (Table 5) showed greater affinity of the adsorbent towards the adsorbate [1]. This is the case for MB-NGT. In addition, it showed increased randomness at the solid/solution interface. The adsorbed solvent molecules, which are displaced by the adsorbate, gained more translational entropy than is lost by the adsorbate, thus allowing for the prevalence of randomness in the system [34]. Opposite trend is observed for MB-SGT, EY-NGT and EY-SGT where entropy change is negative, indicating less randomness at the solid/solution interface.

The values of the isosteric heat of adsorption (ΔHr) (Table 5) were > 40 kJ/mol for EY-NGT and EY-SGT, illustrating a chemisorption mechanism also taking part in the process (Muhammad *et al*., 2014). For adsorption of MB onto both adsorbents, ΔHr values were < 40 kJ/mol, indicating that some element of physical adsorption is greatly involved the adsorption process [1], [32], [34]. On the basis of thermodynamic studies of the adsorption of MB and EY onto NGT and SGT, it can be concluded that the process was feasible, spontaneous, exothermic (except MB-NGT) and proceeded by a combined physisorption and chemisorption mechanism for EY onto both adsorbents while that of MB onto the adsorbents is said to be characterized greatly by some element of physisorption.

Conclusion

This study was focused on the kinetics and thermodynamic modeling of the adsorption of EY and MB onto natural goethite (NGT) and synthetic goethite (SGT) particles. From the adsorption data, the sorptive property of the adsorbents was found to be dependent on time and temperature, with SGT demonstrating a relatively higher adsorption capacity perhaps. That is, NGT could not compete favourably with SGT for decontamination of the dyes from aqueous system. The fittings into the various tested kinetics models are in the order; pseudo-second order > Elovich > second order > pseudo-first order, suggesting that chemisorption was involved in the adsorption processes. For the diffusion models, Weber-Morris showed a better fitting but only slightly. Result of thermodynamics study showed that the

process was feasible, spontaneous and exothermic (except MB-NGT) in nature. Also, the adsorption of EY onto both goethite forms could follow a combined chemisorption and physisorption processes while that of MB onto both adsorbents could be physical in nature as suggested by the magnitudes of ΔH and ΔHr. The combined results of kinetics and thermodynamic studies revealed that the adsorption proceeded by a combined physisorption and chemisorption processes. Additionally, the mechanism of the adsorption occurred by the two processes (intra-particle and film diffusion) simultaneously or that other processes occurred concurrently with these two processes. For future studies, the equilibrium studies, the usability of natural goethite (NGT) and synthetic goethite (SGT) for dyes removal from real industrial effluent will be tested and as comparison, a fixed bed column will be employed to investigate the effect of reactor design.

Conflict of Interest

The authors declare no conflict of interest.

References

[1] A.A. Muhammad, U.F. Audu, A.A. Pam and S.A. Onakpa, Thermodynamic study of the competitive adsorption of chromium (iii) ions and halides onto sweet orange (citrus sinensis) peels as adsorbent, *J. Environ. Anal. Chem*, 1, 2: 114 (2014). Doi:10.4172/JREAC.1000114

[2] M.A. Funtua and F.A. Ugbe, Adsorption of heavy metals from aqueous waste water using unmodified and ethylenediaminetetraacetic acid (EDTA) modified maize cobs, *International Journal of Current Research in Biosciences and Plant Biology*, 2,1: 98 – 103 (2015).

[3] A.O. Dada, F.A. Adekola, E.O. Odebunmi, F.E. Dada, O.M. Bello, B.A. Akinyemi, O.S. Bello and O.G. Umukoro, Sustainable and low-cost *Ocimum gratissimum* for biosorption of indigo carmine dye: kinetics, isotherm, and thermodynamic studies, *International Journal of Phytoremediation*, 1-14: (2020). https://doi.org/10.1080/15226514.2020.1785389

[4] A.H. Mohamed and E. Ahmed, Health and environmental impacts of dyes: Mini Review. *American Journal of Environmental Science and Engineering*, 1, 3: 64-67 (2017).

[5] R.D. Saini, Textile organic dyes: polluting effects and elimination methods from textile waste water, *International Journal of Chemical Engineering Research*, 9, 1: 121-136, (2017).

[6] L. Luo, X. Wu, Z. Li, Y. Zhou, T. Chen, M. Fan, and W. Zhao, Synthesis of activated carbon from biowaste of fir bark for methylene blue removal, *R. Soc. open sci*., 6: 190523 (2019).

[7] F.A. Ugbe and V.A. Ikudayisi, The kinetics of eosin yellow removal from aqueous solution using pineapple peels, *Edorium Journal of Waste Management*, 2: 5 – 11 (2017).

[8] Y. Kuang, X. Zhang, and S. Zhou, Adsorption of methylene blue in water onto activated carbon by surfactant modification, *Water*, 12, 587: 1-19 (2020).

[9] R.R. Elmorsi, S.T. El-Wakeel, W.A.S. El-Dein, H.R. Lotfy, W.E. Rashwan, M. Nagah, S.A. Shaaban, S.A.S. Ahmed, I.Y. El-Sherif and K.S. Abou-El-Sherbini, Adsorption of methylene blue and pb^{2+} by using acid-activated *posidonia oceanica* waste, *SCIENtIFIC REPORTS* 9: 3356 (2019).

[10] A. Arunachalam, R.G. Chaudhuri, E. Iype and B. G. P. Kumar, Surface modification of date seeds (Phoenix dactylifera) using potassium hydroxide for wastewater treatment to remove azo dye, *Water Practice & Technology*, 13, 4: 860 – 870 (2018).

[11] T.S. Anirudhan and S.R. Rejeena, Photocatalytic degradation of eosin yellow using poly (pyrrole-co-aniline)-coated TiO_2/Nanocellulose composite under solar light irradiation, *Journal of Materials*, 2015: (2015). Article ID 636409 | 11 pages | https://doi.org/10.1155/2015/636409

[12] L. Borah, M. Goswami, P. Phukan, Adsorption of methylene blue and eosin yellow using porous carbon prepared from tea waste: Adsorption equilibrium, kinetics and thermodynamics study, *Journal of Environmental Chemical Engineering*, 565: 565 1–11 (2015).

[13] J.O. Amode, J.H. Santos, Z.M. Alam, A.H. Mirza, and C.C. Mei, Adsorption of methylene blue from aqueous solution using untreated and treated (*Metroxylon spp.*) waste adsorbent: equilibrium and kinetics studies, *Int J Ind Chem*., 7:333–345 (2016).

[14] P.O. Anebi, F.A. Ugbe and V.A. Ikudayisi, Equilibrium, kinetics and thermodynamic properties of methylene blue adsorption by termite mound, *Chem. Soc. Nigeria Conf. Proc. 39th Annual Conf*., 57-62 (2016).

[15] A.O. Dada, F.A. Adekola, E.O. Odebunmi, A.A. Inyinbor, B.A. Akinyemi and D. Ilesanmi, Kinetics and thermodynamics of adsorption of rhodamine B onto bentonite supported nanoscale zerovalent iron nanocomposite. *J Phys Conf. Ser.* 1299: 012106 (2019a).

[16] O.S. Bello, K.A. Adegoke, S.O. Fagbenro and S.O. Lameed, Functionalized coconut husks for rhodamine-B dye sequestration. *Appl Water Sci.* 9, 8: 189 (2019).

[17] Nigerian mining sector, *KPMG*, (2012) 1-18, retrieved 19/06/2015.

[18] H. Liu, T. Chen and R.L. Frost, An overview of the role of goethite surfaces in the environment, *Chemosphere*, 103: 1-11 (2013).

[19] X. Wang, N. Chen and L. Zhang, Enhanced Cr (VI) immobilization on goethite derived from an extremely acidic environment, *Environ. Sci. Nano*, 6: 2185 – 2194 (2019).

[20] R. Nayak, and J.R. Rao, Synthesis of active goethite and maghemite from scrap iron sources, *Journal of scientific and industrial research*, 64: 35 – 40 (2005).

[21] G.H. Lee, S.H. Kim, B. J. Choi and S.H. Huh, Magnetic properties of needle-like α-FeOOH and γ-FeOOH nanoparticles, *Journal of the Korean Physical Society*, 45, 4: 1019-1024 (2004).

[22] N. Abdus-Salam, F.A. Ugbe and M.A. Funtua, Characterization of synthesized goethite and natural goethite sourced from Itakpe in North Central, Nigeria, *ChemSearch Journal,* 9, 2: 24 – 32 (2018).

[23] N. Abdus-Salam and F.A. Adekola, The influence of pH and adsorbent concentration on adsorption of lead and zinc on a natural goethite, *Ife Journal of Science*, **7**,1: 131 – 137 (2005).

[24] M. Ladan, A.M. Ayuba, U. Bishir, A. Jamilu and S. Habibu, Thermodynamic properties of chromium adsorption by sediments of River Watari, Kano State, *Chemsearch Journal,* 4: 1 – 5 (2013).

[25] M.B. Ibrahim and W.L.O. Jimoh, Adsorption studies for the removal of Cr (VI) Ion from aqueous solution, *Bayero Journal of Pure and Applied Sciences*, 1, 1: 99 – 103 (2008).

[26] S. Lagergren, About the theory of so-called adsorption of soluble substances. *Kungliga Svenska Vetenskapsakademiens Handlingar*, 24, 4: 1-39 (1898).

[27] Y.S. Ho, and G. McKay, Pseudo Second Order Model for Sorption Processes, *Process Biochemistry*, 34: 451–465 (1999).

[28] G.M. Xu, Z. Shi and J. Deng, Adsorption of antimony on IOCS: kinetics and mechanisms, *Acta Scientiae Circumstantiae*, 26, 4: 607-612 (2006).

[29] Y.S. Ho, Review of second-order models for adsorption systems, *Journal of Hazardous Materials*, 136, 3: 103 – 111 (2006).

[30] W.J. Weber and J.C. Morris, Kinetics of adsorption on carbon from solutions, *Journal of Sanitation Division, American Society of Civil Engineering*, 89: 319 (1963).

[31] G.E. Boyd, A.W. Adamson and L.S. Meyers, The exchange adsorption of ions from aqueous solution by organic zeolites II Kinetics, *Journal of American Chemical Society*, 69: 2836 –2848 (1947).

[32] F.A. Ugbe, A.A. Pam and A.V. Ikudayisi, Thermodynamic properties of chromium (iii) ion adsorption by sweet orange(*citrus sinensis*) peels, *American Journal of Analytical Chemistry*, 4, 5: 666-673 (2014).

[33] M.A. Al-Anber, Thermodynamics approach in the adsorption of heavy metals. *thermodynamics - interaction studies - solids, liquids and gases*, Dr. Juan Carlos Moreno PirajÃ¡n (Ed.), 738-761 (2011).

[34] Saha and S. Chowdhury, Insight into adsorption thermodynamics. *InTech*, 16: 350-364 (2011).

[35] J. Gim´enez, M. Mart´ınez, J. Pablo, M. Rovira and L. Duroc, Arsenic sorption onto natural hematite, magnetite, and goethite, *Journal of Hazardous Materials*, 141: 575 – 580. (2007).

[36] S.M. Kanawade and R.W. Gaikwad, Removal of methylene blue from effluent by using activated carbon and water hyacinth as adsorbent, *International Journal of Chemical Engineering and Applications*, 2, 5: (2011).

[37] M.A. Zulfikar, H. Setiyanto and S.D. Djajanti, Effect of temperature and kinetic modelling of lignosulfonate adsorption onto powdered eggshell in batch systems. *Songklanakarin Journal of Science and Technology*, 35, 3: 309 – 16 (2013).

[38] M.S. Eldin, K.M. Aly, Z.A. Khan, A.M. Mekky, T.S. Saleh and A.S. Al- Bogami, Removal of methylene blue from synthetic aqueous solutions with novel phosphoric acid-doped pyrazole-g-poly(glycidyl methacrylate) particles: kinetic and equilibrium studies, *Desalination and Water Treatment*, 1–16 (2016).

[39] U.A. Edet and A.O. Ifelebuegu, Kinetics, isotherms, and thermodynamic modeling of the adsorption of phosphates from model wastewater using recycled brick waste, *Processes*, 8, 665: 1-15 (2020).

[40] Y.S. Ho and G. McKay, A Comparison of chemisorptions kinetic models applied to pollutant removal on various sorbents, *Process Safety and Environmental Protection*, 76:4 332 – 340 (1998).

[41] H.I. Adegoke, F.A. Adekola, O.S. Fatoki and B.J. Ximba, Adsorption of Cr (VI) on synthetic hematite (α-Fe_2O_3) nanoparticles of different morphologies, *Korean Journal of Chemical Engineering*, 31, 1: 142 – 154 (2013).

[42] J.T. Utsev, R.T. Iwar and K.J. Ifyalem, Adsorption of methylene blue from aqueous solution onto delonix regia pod activated carbon: batch equilibrium isotherm, kinetic and thermodynamic studies, *J. Mater. Environ. Sci*., 11, 7: 1058-1078 (2020).

[43] P. Pandey, S.S. Sambi, S.K. Sharma and Surinder, Batch adsorption studies for the removal of Cu (II) ions by zeolite NaX from aqueous stream, *Proceedings of the World Congress on Engineering and Computer Science*, 1, San Francisco, USA (2009).

[44] Y. Sağ and Y. Aktay, Kinetic studies on sorption of Cr (vi) and Cu (ii) ions by chitin, chitosan

and rhizopus arrhizus. *Biochemical Engineering Journal*, 12, 2: 143-153 (2002).

[45] P.V. Nidheesh, R. Gandhimathi, S.T. Ramesh and T.S.A. Singh, Kinetic analysis of crystal violet adsorption on to bottom ash, *Turkish Journal of Engineering and Environmental Science*, 36: 249 – 62 (2012).

[46] A. Mittal, K. Lisha and M. Jyoti, Freundlich and Langmuir adsorption isotherms and kinetics for the removal of Tartrazine from aqueous solutions using hen feathers. *Journal of Hazardous Materials* 146: 243–248 (2007).

[47] A. M. Gamal, S. A. Abo-Farha, H. B. Sallam, G. E. A. Mahmoud, and L. F. M. Ismail, Kinetic study and equilibrium isotherm analysis of reactive dyes adsorption onto cotton fiber, *Nature and Science*, 8,11: 95-110 (2010).

[48] P. Zhanga, D. Connora, Y. Wang, L. Jiang, T. Xiab, L. Wanga, D.C.W. Tsangc, Y.S. Okd, and D. Houa, A green biochar/iron oxide composite for methylene blue removal. *Journal of Hazardous Materials*, 384:121286 (2020).

[49] M. El Marouani, K. Azoulay, I. Bencheikh, L. El Fakir, L. Rghioui, A. El Hajji, S. Sebbahi, S. El Hajjaji and F. Kifani-Sahban, Application of raw and roasted date seeds for dyes removal from aqueous solution, *J. Mater. Environ. Sci.*, 9, 8: 2387-2396 (2018).

[50] H. K. Boparai, M. Joseph and D. M. O'Carroll, Kinetics and thermodynamics of cadmium ion removal by adsorption onto nano zerovalent iron particles. *Journal of Hazardous Materials*, 2010: 1-8 (2010).

[51] R. Prabakaran and S. Arivoli, Adsorption kinetics, equilibrium and thermodynamic studies of Nickel adsorption onto *thespesia populnea* bark as biosorbent from aqueous solutions, *European Journal of Applied Engineering and Scientific Research*, 1, 4:134-142 (2012).

[52] S. Rattanaphani, M. Chairat, J.B. Bremner and V. Rattanaphani, An adsorption and thermodynamic study of lac dyeing on cotton pretreated with chitosan, *Dyes and Pigments*, 72: 88-96 (2007).

[53] S. Chatterjee, S. Chatterjee, B. Chatterjee, A. Das and A. Guha, Adsorption of a model anionic dye, eosin Y, from aqueous solution by chitosan hydrobeads, *Journal of Colloid and Interface Science*, 288: 30 –35 (2005).